

# New frontiers in hybrid materials: noble metal nanoparticles – supramolecular gel systems

Massimo Cametti\*<sup>a</sup> and Zoran Džolić\*<sup>b</sup>

Received 3rd February 2014,

Accepted 18th March 2014

## 1. Introduction

A major challenge in modern chemistry is the search for novel materials for advanced applications.<sup>1</sup> In this respect, metal nanoparticles (NPs) have surely inspired material chemists and physicists during recent decades due to their surprising optical, electronic, magnetic and catalytic properties,<sup>2</sup> with vast potential in many fields of application.<sup>3</sup> As their physico-chemical attributes derive mainly from particle size and shape and inter-particle distance, the properties of NPs are different

from those of bulk materials, and from those of molecular compounds. Nowadays, the synthesis and characterization of NPs are well established techniques, but, perhaps surprisingly, NPs are not a discovery of modern science, as they have been identified in artifacts and works of art from Roman times, especially mosaics, and they were already employed in glass manufacturing by proto-historic communities during the Bronze Age.<sup>4</sup>

Over the last decade, a very original line of research has focused on the attempt to integrate NPs into unconventional environments, with the aim of producing hybrid materials. The coupling of material systems belonging to different dimensional scales into integrated novel composites is an exciting area of research. In particular, the integration of nano-objects within micro environments would eventually generate materials of macro dimensions whose properties

<sup>a</sup> Department of Chemistry, Materials and Chemical Engineering "Giulio Natta", Politecnico di Milano, Via Mancinelli 7, I-20131, Milan, Italy.

E-mail: massimo.cametti@chem.polimi.it

<sup>b</sup> Ruđer Bosković Institute, Bijenička c. 54, 10000 Zagreb, Croatia.

E-mail: Zoran.Dzolic@irb.hr

might open new perspectives from the applicative and technological points of view.

If precise control of the process of transcription of chemical information from the molecular to the macroscopic level is feasible, complex functional materials can be assembled from simple building blocks.<sup>5</sup> When both organic and inorganic units are employed, the resultant composites may possess advantages offered by the combination of complementary strengths, and by the synergy between the properties of components derived from different chemical domains. This approach is significant not only for the design of nanodevices, but also for the fundamental understanding of the collective properties which may arise from inter-component interactions within the final composite assembly. The organization of NPs into well-defined and easily reproducible 2- and 3-D architectures is a particularly promising route not only for the construction of optoelectronic and biomedical devices, but also for the discovery of novel physico-chemical properties of organized matter. In order to explore these possibilities, a variety of strategies have been undertaken. A particularly promising one focuses on gel systems, which have attracted considerable interest in this respect. Indeed, the past decade has witnessed an increased interest in the development of gel systems as structural partners for noble metal NPs, giving rise to unique novel materials: NPs–gel systems.

Gels are soft materials generated by the entrapment of large quantities of solvent within a reticulated superstructure made of intertwined fibrils of varying dimensions, which constitutes only a tiny fraction of the overall mass of the system (<1%).<sup>6a</sup> Gels can be of chemical or physical nature, polymeric or generated by low molecular weight gelator (LMWG) molecules. The latter category has attracted significant attention due to the ever-increasing possibility that a fully supramolecular approach can indeed be achieved.<sup>6,7</sup> A non-covalent approach enables the construction of materials with a fine design and precise organization just above the molecular level. Moreover, non-covalent bonds are reversible and more susceptible to the environment, thus their use paves the way to adaptable and stimuli responsive materials. Despite the superior intrinsic robustness of polymeric gels and the ease in their mechanical manipulation,<sup>8</sup> cross-linking reactions do not allow for fine control of the material's internal structure.

As this review intends to demonstrate, LMWG gel systems can indeed be advantageous for achieving the assembly of objects belonging to different dimensional domains into functional materials. Indeed, integrated NPs–gel systems consist of a combination of nanoscale objects, *i.e.*, the incorporated NPs, and micrometer-scale gel-fibers, all of them assembled into a macroscopic material. Most interestingly, the distribution of NPs within the composite material might be far from homogeneous. This strongly depends on the gel morphology and, thus, the final properties of the nanoscale objects within the macroscopic materials might be modulated by the microscopic features of the gel's internal structure.

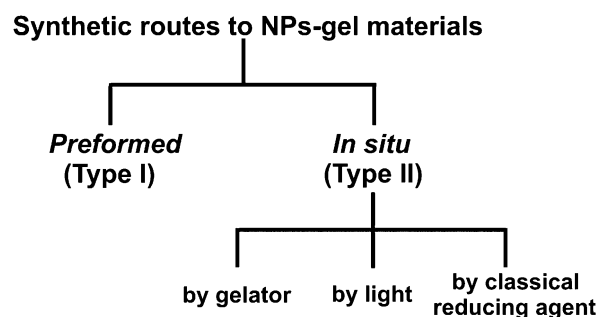
This review article presents an account of the works related to the emerging field of supramolecular NPs–gel materials.

Extensive discussions and numerous reviews on each separate structural element constituting these novel hybrid materials, *viz.*, LMWG gel systems and NPs, already exist in the literature.<sup>9</sup> Therefore, here we will focus on the general aspects pertaining to the design of supramolecular NPs–gel systems and to the different methods of their preparation. To this end, we have selected prime examples which describe how these novel materials can be produced. The variables involved in the preparation of NPs–gel materials require attention in order to outline common procedural features. Despite the rather large chemical variety of the species considered in this review, it was quite feasible to identify two main categories of works according to the synthetic pathway used in the material preparation. We also describe the structural and optical features of these novel materials, which are usually investigated by physico-chemical tools (TEM, SEM, AFM, surface plasmon resonance (SPR), X-ray powder diffraction, *etc.*). In general, most of the research studies reported in this review look into the effects that the entrapment of pre-formed NPs into a gel environment has on their properties, or into the effect that gelator molecules and their assembly exert on the formation and on the final stability of the NPs. Moreover, they are actually carried out with the aim of specifically improving one of the two components (*viz.*, the gel or the NPs) by the effect exerted by the presence of the other one in the composite. At odds with this *narrow* view, we and others strongly believe that the resulting materials can be thought of as integrated systems which could lead to novel materials with unprecedented properties. Hence, the second part of this work is dedicated to displaying some of the most interesting practical uses that can be attained by NPs–gel systems.

## 2. Preparation and characterization of NPs–gel composites

There are a number of ways to produce NPs–gel composites. For simplicity's sake, we grouped the most interesting works into two main categories (Scheme 1) based on whether the NPs are formed prior to the assembly of the hybrid material (type I) or by an *in situ* process (type II).

While the type I group includes procedures in which the NPs are prepared by classical methods<sup>10</sup> and integrated into the gel



Scheme 1 Different categories of NPs–gel material based on the preparation procedure used.

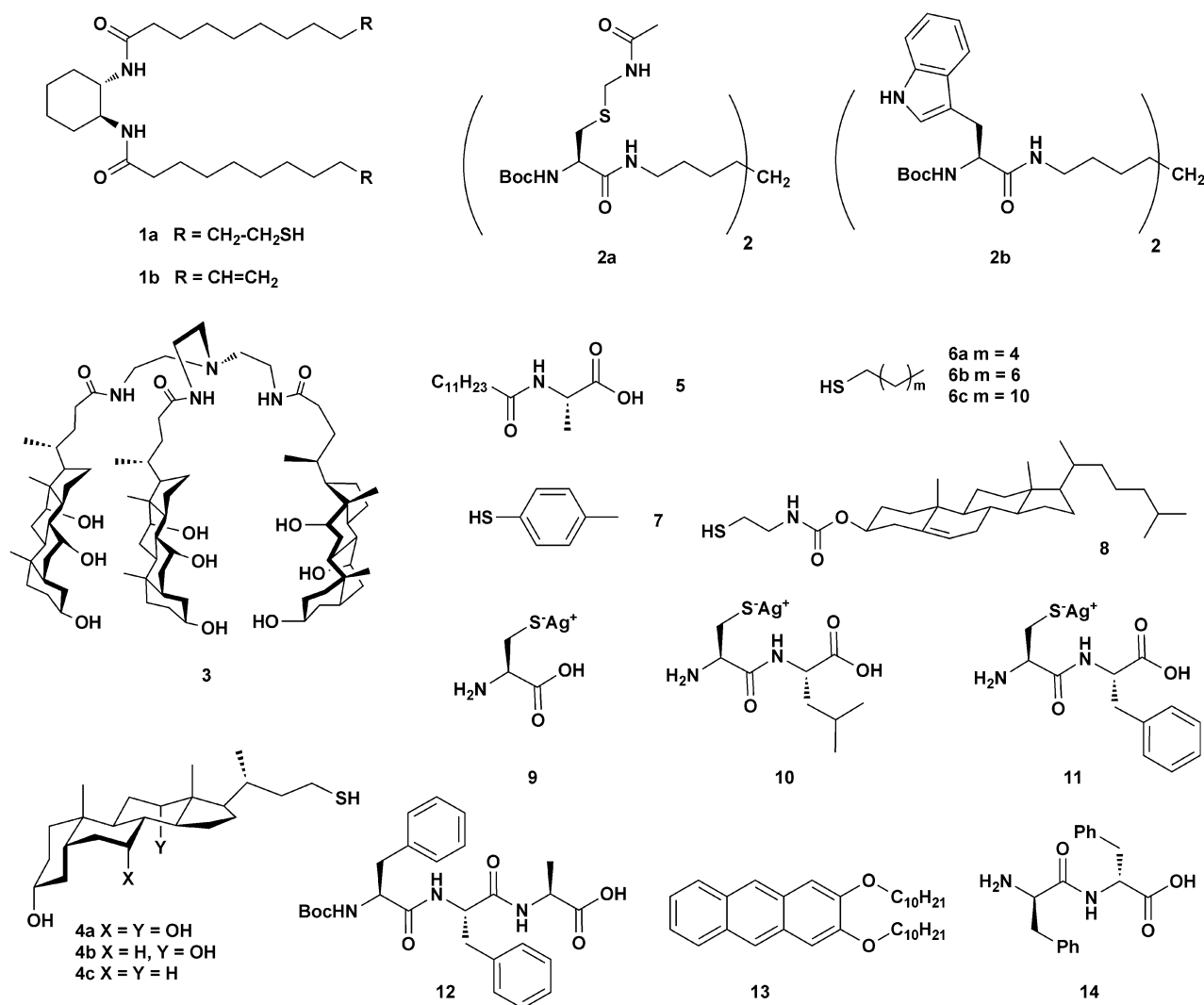
matrix afterwards, in the examples of the type II group the NPs are generated by *in situ* reduction, by chemical or physical stimuli, within the gel material or during its formation. The latter group includes reduction processes based on light absorption, or by chemical reduction achieved by the gelator molecules themselves or by classical reducing agents ( $\text{NaBH}_4$ , *etc.*). As the reader might easily imagine, these two methods achieve different outcomes. Indeed, while the type I process embeds into the gel matrix NPs whose intrinsic properties are largely pre-determined, the type II procedure partially empowers the gel formation process itself to determine the final NPs' characteristics. Another key aspect is the type of chemical protective coverings (termed capping agents) employed in synthesis of the NPs. While they are necessary to ensure prolonged stability of the NPs and avoid their aggregation,<sup>11</sup> capping agents also provide additional variability and interest to these systems. Not only that, they mediate the interactions between the NPs and their surroundings, thus representing a functional interface.

## 2.1 Type I: use of pre-formed NPs

NPs tend to be fairly unstable in solution, and precautions must be taken in order to avoid aggregation phenomena. Organic monolayers are generally used as capping agents to passivate the NPs surface and prevent precipitation. A viable integration of NPs into the gel material is dependent on a proper communication between the chemical covering of the NPs and the external environment based on chemical affinity.

The strong interaction that can be established between noble metals NPs and thiol groups can be essential in order to obtain NPs-gel materials. As described by Kimura, Shirai and co-workers,<sup>12</sup> gelator **1a** (Scheme 2), despite its reduced gelling ability compared to the parent **1b** (Scheme 2), can still produce gel materials in several polar and apolar systems. Its two thiol units may be used as anchoring points for octanethiol-stabilized gold nanoparticles ( $1.7 \pm 0.3 \text{ nm } \varnothing$ ,  $\text{SPR}_{\text{max}} = 512 \text{ nm}$ ), synthesized independently by the classical Brust method.<sup>10</sup>

A heated solution of **1a** in degassed toluene in the presence of octanethiol-stabilized AuNPs produced a gel upon cooling.



Scheme 2 Molecular formulae for compounds 1–14.

TEM analysis revealed the presence of spatially organized AuNPs assembled onto the gel fibers (80–400 nm  $\varnothing$ ). The better gelator, **1b**, was unable to generate the composite material. A site-exchange mechanism operates, and a number of capping agents, originally on the NPs, are replaced by the gelator thiol groups. The lack of –SH groups in **1b** precluded the essential direct gelator–NPs interaction.

The same concept underlies the work of Smith *et al.*, which reported the stabilization and organization of AuNPs by the cysteine-functionalised organogelator **2a** (Scheme 2).<sup>13</sup> In the presence of AuNPs, **2a** formed a gel material in toluene, on whose fibers (75–200 nm  $\varnothing$ ) the nanoparticles were aligned, as shown by the TEM images (Fig. 1a).

Most interestingly, the coverage of NPs on the fibers was found to be dependent on the capping agent used, *viz.*, either octadecylsulfide (ODS) or hexadecylthiol (HTD). The replacement of capping thiols with the organogelator **2a**, *via* a ligand exchange mechanism, occurred in both cases, but ODS showed a lesser degree of substitution, shown by the more effective coating of the gel fibers by NPs when HTD cappings were employed. Further confirmation of the actual active role of the sulfur atom in **2a** was given by the outcome of a control experiment with a tryptophan functionalised gelator **2b** (Scheme 2).

This species was ineffective in the organization of NPs. The authors cleverly also measured the average size of the AuNPs after the formation of the NPs–gel material, and they found a slight shift in the NPs' size distribution (from  $2.8 \pm 0.8$  to  $2.1 \pm 1.0$  nm  $\varnothing$ ), which might indicate some reorganization occurring during the formation of the new material. In principle, the gel forming process could have an influence on pre-formed NPs as well, but this aspect is seldom investigated, and the previous study, to the best of our knowledge, is one of only two cases in which this additional study was performed.

A different strategy, which focuses on the capping ligands as interaction mediators between the NPs and the gelator, is exemplified by the following interesting works. The tripodal bile-acid gelator **3** (Scheme 2) is known to form gels in an AcOH–H<sub>2</sub>O mixture (fibers of 50 nm  $\varnothing$ ). Capping agents such as **4a–c** (Scheme 2) were envisaged to be able to interact with **3**,<sup>14</sup> in view of the well documented self-aggregation tendency of facially amphiphilic steroids. Indeed, while AuNPs capped with **4a–c** agents (1.5–3.5 nm  $\varnothing$ , SPR<sub>max</sub> = 520 nm) were found to be unstable in an AcOH–H<sub>2</sub>O mixture, they showed no sign of degradation within the gel materials made from **3**. TEM images show a regular arrangement of the NPs on the top of (and possibly inside) the gel fibers (Fig. 1b).

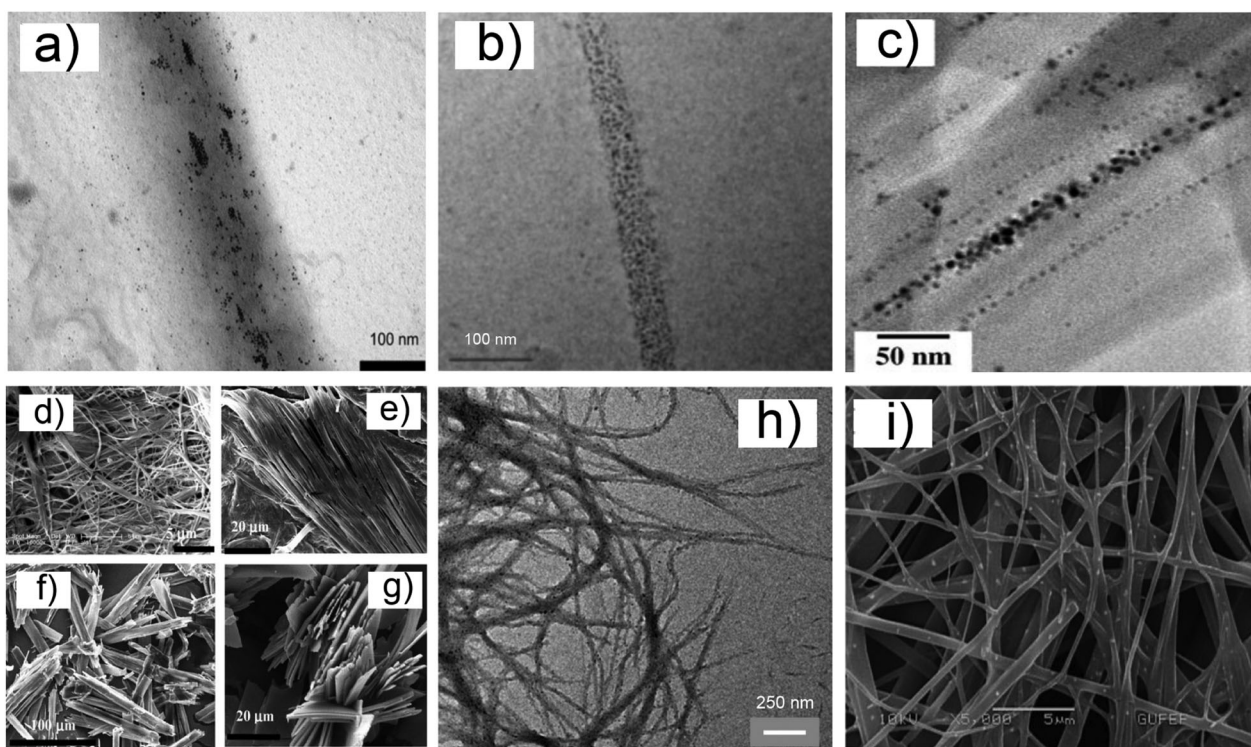


**Fig. 1** SEM and TEM images of NPs–gel systems. (a) TEM image of AuNPs stabilized by ODS and interacting with the fibers of **2a**, from ref. 13; (b) TEM image of AuNPs stabilized by **4a** and interacting with fibers of **3**, from ref. 14, reproduced with permission, Copyright © (2006) American Chemical Society; (c) TEM image of AuNPs stabilized by **7** and interacting with gel fibers of **5**, from ref. 15b, reproduced with permission, Copyright © 2009, WILEY-VCH Verlag GmbH & Co; (d) SEM image of xerogels of **5**, and of the hybrids **6c**-capped NPs–gel (e), **7**-capped NPs (f) and **8**-capped NPs (g), from ref. 15a, reproduced with permission, Copyright © 2006, WILEY-VCH Verlag GmbH & Co; (h) TEM image of AgNPs stabilized by **11** and interacting with gel fibers made of **12**, ref. 16, reproduced with permission, Copyright © (2012) American Chemical Society; (i) SEM image of AuNPs stabilized by fluororous thiols HSR (R = C<sub>2</sub>H<sub>4</sub>–C<sub>8</sub>F<sub>17</sub>) and interacting with gel fibers made of Phe–Phe **14**, from ref. 18, reproduced with permission, Copyright © (2013) American Chemical Society.

Bhattacharya and co-workers focused on a different gelator system, the *N*-lauroyl-L-alanine **5** (Scheme 2), which has already been the subject of extensive studies of its gelation properties of hydrocarbons (fibers of 50–100 nm  $\varnothing$ ). The gel system provided a basis for a systematic study<sup>15</sup> aimed at recognizing the effect of the conspicuous presence of NPs well within the gel matrix, as observed from the TEM image for the example shown in Fig. 1c, on the properties of the gel. Effort was made to identify the influence that capping agents may exert on the morphological features and viscoelastic properties of the AuNPs–gel nanocomposites. Different sets of capping agents were used, e.g., 4-, 6-, and 10-carbon long alkyl- and aromatic thiols, **6a–c** and **7**, and bile-acid derivative **8** (Scheme 2). SEM analyses showed that gel fibres made of **5** behaved in a considerably different manner depending on the capping agents covering the NPs ( $3.0 \pm 0.8$  to  $6 \pm 1$  nm  $\varnothing$ ,  $\text{SPR}_{\text{max}} = 500\text{--}525$  nm). Upon addition of AuNPs stabilized by the aliphatic thiols **6a–c**, the gel reshaped into a thick network of collated fibers, while “rolled-tubular” aggregates formed upon addition of NPs capped with the cholesterol derivative **8**. Such morphologies, which also display thicker fibers, indicate increased fiber–fiber interactions induced by the presence of the NPs. Finally, 7-capped AuNPs generated less dense, platelet-like structures (see Fig. 1d–g). Rheological studies performed on the composites showed that the incorporation of alkanethiol- and cholesterolthiol-capped AuNPs (**6a–c** and **8**) improved the rigidity of the gel (higher yield stress values were observed). On the other hand, 7-capped AuNPs slightly decreased the rigidity. This data set clearly demonstrates the importance of the gelator–capping agent relationship.

Banerjee and co-workers<sup>16</sup> recently reported on the modulation of the mechanical properties of hybrid hydrogel materials by incorporating AgNPs capped with cysteine (Cys, **9**) and the cysteine-based dipeptides Cys–Leu (**10**) and Cys–Phe (**11**) (Scheme 2). The N-terminally protected tri-peptide **12** (Scheme 2) produces a stable supramolecular hydrogel (fibers of 80–150 nm  $\varnothing$  by SEM). Cysteine-based capping ligands have two functions: the cysteine fragment stabilizes the AgNPs (2.4–4.5 nm  $\varnothing$ ), and the adjacent residue interacts with the hydrogelator molecules through hydrophobic interactions. Morphological studies of the hybrid hydrogel by TEM (Fig. 1h) confirmed the presence of AgNPs, mainly along the hydrogel nanofibers. The mechanical strength of the gel can be modulated by varying the nature of the capping ligands, similar to that seen in the previous examples, but also by varying the size and the amount of NPs employed. Increasing the total surface area of the NPs (by adding more NPs or by increasing their size) invariably leads to diminished gelator–gelator interactions, which, in turn, lower the gel strength in all cases.

A similar behavior was also observed by Del Guerzo and co-workers, who noticed a gradual decrease in the stiffness of an organogel material made of the anthracene derivative **13** in *n*-butanol upon addition of increasing amounts of AuNPs.<sup>17</sup> While the presence of the AuNPs (*ca.* 3 nm  $\varnothing$ ,  $\text{SPR}_{\text{max}} = 500$  nm), capped with different linear alkyl- and perfluoroalkyl-thiols ( $\text{C}_6\text{H}_{13}$ ,  $\text{C}_{12}\text{H}_{25}$  and  $\text{C}_2\text{H}_4\text{--C}_8\text{F}_{17}$ ), did not alter the morphology

of the gel fibers (100–200 nm  $\varnothing$ ), the hosted NPs did have a dramatic effect on the fluorescence of the gelator molecule, in a manner that shows some degree of proportionality with the concentration of NPs. Indeed, the observed optical response, which is linear for  $<10^{-5}$  molar ratios of NPs, suggests a regular decrease in the inter-particle distance, simply obtained by diluting the content of NPs.

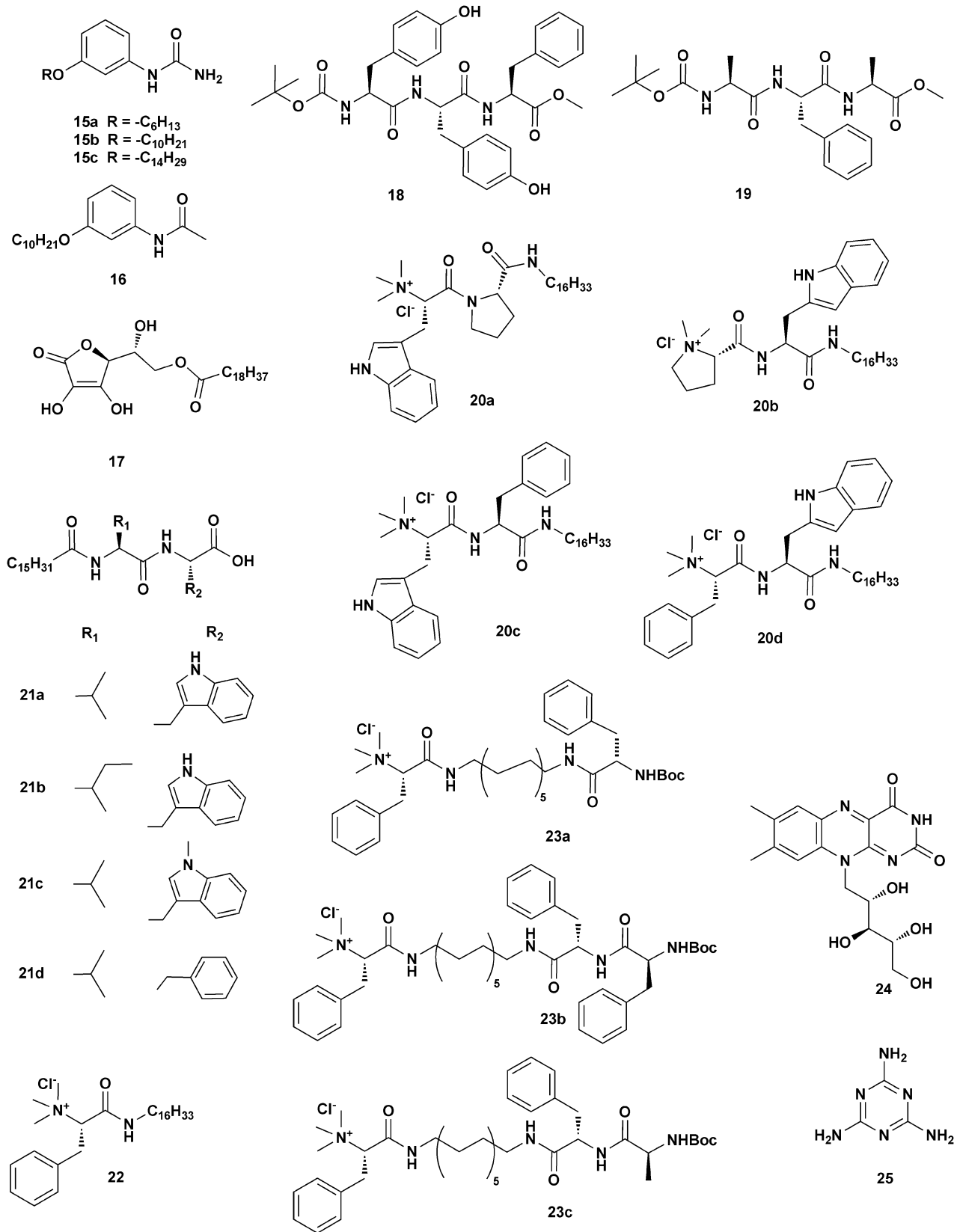
A final example reveals an interesting relationship between NPs’ dimensions and gel morphology. When a chloroform solution of AuNPs – pre-formed by classical reduction methods in the presence of sodium citrate – is added to a solution of diphenylalanine (Phe–Phe) dipeptide **14** in hexafluoropropanol, a gel is formed, as reported by Demirel *et al.*<sup>18</sup> A SEM image of the obtained NPs–gel material is shown in Fig. 1i. Interestingly, significant differences in the gel morphology were observed depending on the average size of the NPs employed (10–60 nm  $\varnothing$ ,  $\text{SPR}_{\text{max}} = 495\text{--}533$  nm), as shown by the SEM study. While 10 nm sized NPs did not practically change the original gel structure, increasing the dimensions of the nano-objects (up to 60 nm  $\varnothing$ ) affected the gelator self-assembly process. The authors related this phenomenon to other works on the adhesion of proteins to the surface of NPs, where it was found that flatter NP surfaces can better adsorb proteins. The system can also undergo a laser-triggered gel disruption process. Indeed, illumination of the NPs–gel system by a green laser, whose emission matches the absorption profile of the NPs, led to a transition to solution.

## 2.2 Type II: synthesis of NPs–gel composites under *in situ* conditions

The redox reaction which converts the metal salt of choice into metallic NPs may not necessarily be preformed prior to the gel formation. It could also be achieved *in situ* within the gel material. There exists a certain amount of variability in the procedures which follow this route, and they essentially differ depending on the identity of the active reducing species. Interestingly, several examples demonstrate that the structural features of the gelator molecule itself can act as efficient reducing sites.

John *et al.*<sup>19</sup> described two ways of making hybrid materials in which *in situ*  $\text{HAuCl}_4$  to AuNPs conversion was achieved in the presence of a molecular species capable of acting in two roles: as a gelator and as a reducing agent. In the first case, the authors focused on the mono-substituted urea derivatives **15a–c** (Scheme 3), which are excellent ambidextrous gelators.<sup>19a</sup> In a typical procedure, a mixture of  $\text{HAuCl}_4$  and gelator was heated to 50 °C, then allowed to cool down. The initial change of the solution from yellow to colourless progressed to a pink-coloured gel material at room temperature, which was identified as a AuNPs gel ( $\text{SPR}_{\text{max}} = 553$  nm). SEM and TEM analyses showed an unchanged gel morphology, regardless of the presence of the AuNPs, which were found to be spherical in shape (11–15 nm  $\varnothing$ ) and dispersed mainly on the edges of the gel platelets (Fig. 2a).

Due to the terminal ureidic  $\text{NH}_2$  group, compounds **15a–c** were suggested to be responsible for the reduction of Au(III) to



Scheme 3 Molecular formulae for compounds 15–25.

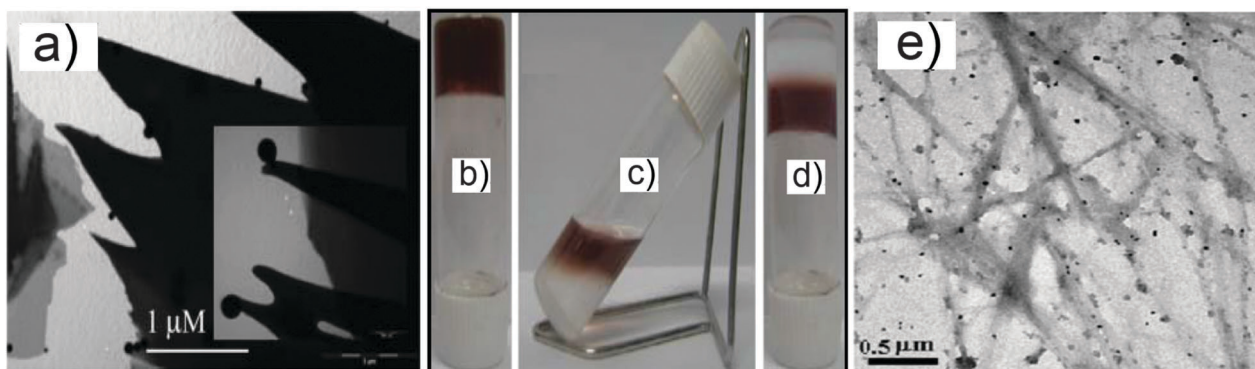


Fig. 2 (a) TEM image and magnification of AuNPs within the gel system made of **15a**, adapted from ref. 19a; (b–d) pictures of the process of the NPs' transfer from the hydrogel to the organogel system of **21a**, and (e) TEM image of the AuNPs embedded in the gel; reproduced from ref. 22.

Au(0). In order to test the above hypothesis, the acetanilide derivative **16** was synthesized (Scheme 3). Under the same conditions, it did form a gel material, but no nanoparticles were detected within it. This fact, however, might not be definitive proof, and an electrochemical investigation on the redox potentials of the system could be helpful in this case.

In the second example, *in situ* synthesis of AuNPs in a gel matrix was accomplished by employing the ascorbic acid derivative **17** (Scheme 3), which can form highly interdigitated bilayer-like gels in water at low concentrations.<sup>19b</sup> The gelator design originates from the ability of ascorbic acid to reduce auric salts to metallic gold and the need of an amphiphilic character (introduced by the alkyl chain) to induce gelation. The addition of **17** to a HAuCl<sub>4</sub> solution, followed by heating, resulted in a change in the solution colour, from yellow to colorless, which then progresses to the formation of a pink gel. The presence of the NPs in the materials was confirmed by the presence of a telltale SPR band in the UV-vis spectrum (SPR<sub>max</sub> = 555 nm). SEM analysis showed that the sheet-like morphology of the gel did not change due to the presence of the AuNPs. Moreover, TEM images revealed that the AuNPs (11–18 nm  $\varnothing$ ) were not assembled along fibers, and rather were uniformly distributed within the gel matrix. Bearing in mind the different behavior described for the systems presented previously, the lack of specific NP–gelator interactions might be responsible for that.

Banerjee and co-workers<sup>20</sup> studied the tripeptide organogelator **18** containing two Tyr residues (Scheme 3). Chloroauric acid was added to a gel made of **18** in a basic 1 : 1 MeOH–water mixture and heated at 50 °C. Once equilibrated at room temperature, the characteristic yellow shade of the AuCl<sub>4</sub><sup>−</sup> species was lost and the gel acquired a bluish-violet color (SPR<sub>max</sub> = 551 nm). AuNPs (15–40 nm  $\varnothing$ ) were formed within the gel matrix. The hypothesis that the Tyr residues acted as the reducing agent was confirmed by the use of the model tripeptide Boc–Ala–Phe–Ala–OMe (**19**, Scheme 3) which was found to be completely ineffective under the investigated conditions.

Similarly, *in situ* syntheses of gold nanoparticles in hydrogels made of the tryptophan-based dipeptide amphiphiles **20a–d** were reported (Scheme 3).<sup>21</sup> It was found that the different

gel morphologies observed for the four gelators was a key factor in the formation of differently sized and shaped AuNPs. Both SPR data and TEM images corroborate the presence of nanosheets, nanowires, nano-octahedra and nano-decahedra NPs (10–200 nm  $\varnothing$ , SPR<sub>max</sub> = 515–688 nm) within the gel matrices.

The same group also reported a very intriguing process in which *in situ* synthesized AuNPs–hydrogel nanocomposites could be converted into an AuNPs–organogel hybrid simply by changing the pH.<sup>22</sup> The system is based on the amphiphilic dipeptides **21a–c** (Scheme 3), containing tryptophan residues, but surprisingly also with the derivative **21d**. In general, these derivatives have an interesting feature: their carboxylate form behaves as a hydrogelator, while the carboxylic acid form acts as an organogelator. The whole process starts with the formation of an AuNPs–hydrogel made by the addition of aqueous HAuCl<sub>4</sub> to preformed **21a–d** hydrogels (under stirring, pH = 9–10) to achieve a final gelator : Au(III) ratio of 10 : 1. Analysis of this material confirmed the presence of AuNPs based on a colour change (Fig. 2b) and the appearance of the SPR band (SPR<sub>max</sub> 523–525 nm). After that, toluene was added to form a biphasic system and aqueous HCl was used to convert the carboxylate into acid. This addition led to a transfer of the gelators into the organic phase, carrying the AuNPs along with them (Fig. 2c). The mixture was eventually gelled with simultaneous NPs entrapment (Fig. 2d). The novel materials were also analyzed by SEM and TEM imaging, X-ray diffraction, fluorescence and rheology. In particular, the TEM images revealed the importance of the supramolecular networks in the stabilization of the nanoparticles in both the hydrogel and the organogel, as the AuNPs (12–14 nm and 15–17 nm for **21a–b** and **21c–d**, respectively) were found to be aligned on the surface of the amphiphilic nanofibers (Fig. 2e). Also, the mechanical strength of the nanocomposite improved, probably due to the formation of denser and more compact fibers. Questions remain as to the rationale on the basis of the behavior of **21d**, which does not possess the reducing tryptophan moiety. Additional comparison with the behavior of simpler systems, and even with a simple linear aliphatic fatty acid (C<sub>16</sub>) – which surprisingly succeeds in the formation of the material, although showing limited NPs formation – indicates that the

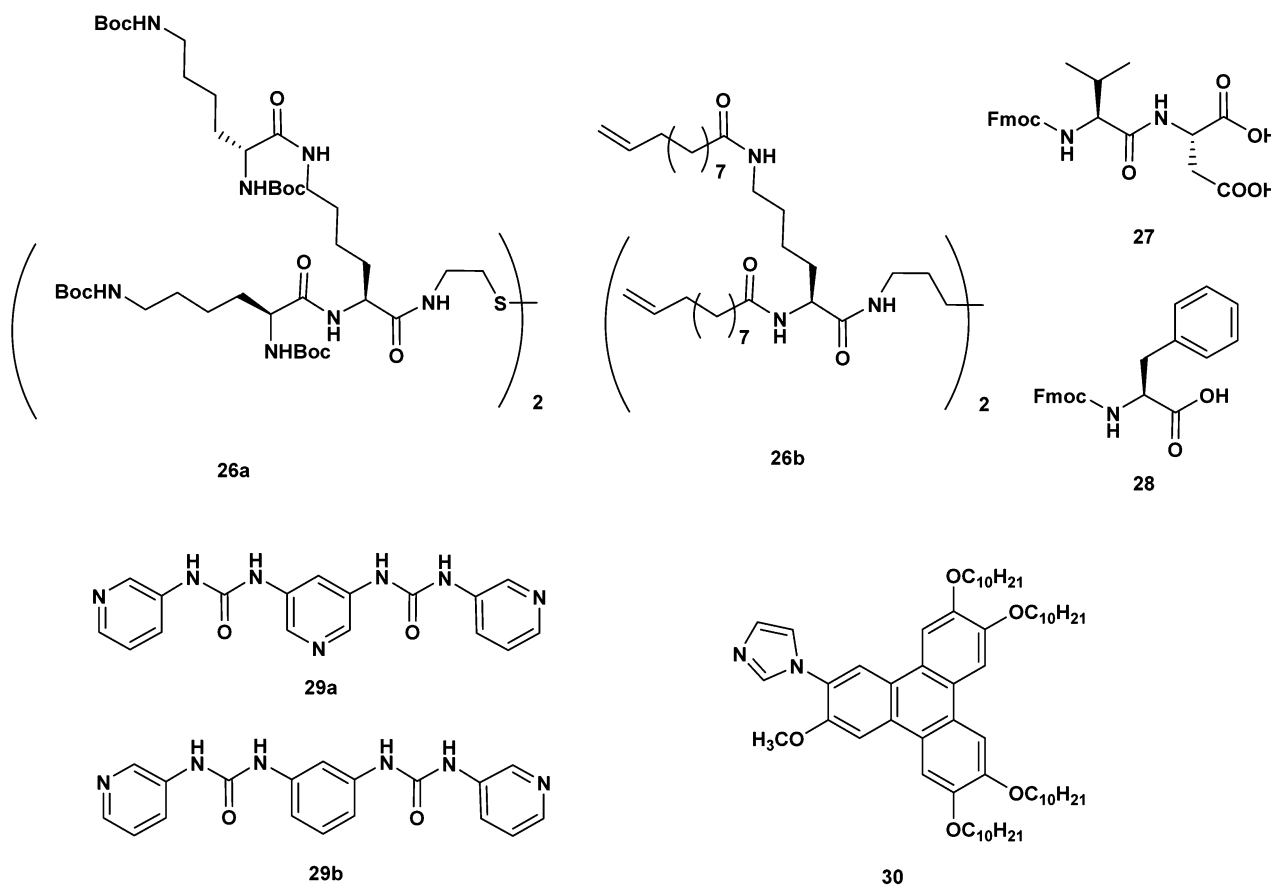
presence of specific reducing moieties, usually considered as essential by some authors, might not be quite so.

Indeed, the latter observation is supported by a recent work mainly related to gelator structural modifications aimed at providing enhanced gelling ability.<sup>23</sup> Here, it has been shown that the *L*-phenylalanine-based poor hydrogelator **22** (Scheme 3), and the more efficient tail-modified amphiphiles **23a–c** (Scheme 3) were capable of the *in situ* synthesis of AuNPs within the gel material without the help of any external reducing agents. Interestingly, the identity of the gelator and its concentration relative to the Au(III) salt dictated the shape and size of the resulting embedded AuNPs (spherical, triangular or polyhedral shapes, 15–45 nm  $\varnothing$ ).

A very interesting example of a bio-inspired system is given by the work of Nandi and co-workers,<sup>24</sup> which investigated the riboflavine (**24**)/melamine (**25**) two-component system with the aim of NPs production (Scheme 3). Mixing different quantities of AgNO<sub>3</sub> powder with a 1 : 1 mixture of **24** and **25** in water, after homogenization at 90 °C, produces a AgNPs–hydrogel composite (the riboflavin moiety acts as the reducing agent). Spectroscopic and electron microscopy techniques reveal a well-defined morphologic transformation of the gel materials: the hollow tubes of the hydrogel are converted either into helical fibers, rod-like structures, or spheroidal aggregates, simply depending on the concentration of metal salt used. Also, the size of the NPs

drastically increases with the amount of AgNO<sub>3</sub> employed in the material production ( $12 \pm 4$  to  $52 \pm 8$  nm  $\varnothing$ , SPR<sub>max</sub> = 535 nm;  $1000 \pm 200$  nm  $\varnothing$ , SPR absent).

Under certain conditions, UV light is capable of reducing metal salts to metallic NPs.<sup>25</sup> One of the first examples of UV light induced formation of gel–NPs materials was presented by Chechik, Smith *et al.*<sup>26</sup> The authors employed a gel material made of the dendritic gelator **26a** in toluene (Scheme 4). Chloroauric acid was transferred into the toluene phase by the use of a phase transfer agent (tetraoctylammonium bromide) and allowed to diffuse into the gel material. Once irradiated with a Hg-lamp, the gel initially changed its colour from yellow to colourless and finally to deep purple in a matter of hours (indicating a two step Au(III)  $\rightarrow$  Au(I)  $\rightarrow$  Au(0) transformation). In this case, the quaternary ammonium salt also acts as a sacrificial reductant species.<sup>27</sup> TEM images of the obtained NPs–gel system confirmed the presence of NPs within the gel matrix (13 nm  $\varnothing$ , SPR<sub>max</sub> = 550 nm). The gelator was found to be essential for nanoparticle formation, since the irradiation of a toluene solution of HAuCl<sub>4</sub> alone resulted in the deposition of bulk elemental gold. Indeed, the gelator acts as a stabilizer for the NPs, as shown by the fact that whenever the gel is disrupted (by heating or by adding MeOH) the NPs collapse into black aggregates. Interestingly, the hypothesis of specific sulfur–gold gelator–NPs interactions can be ruled out,



Scheme 4 Molecular formulae of compounds **26–30**.



since a structurally related gelator **26b** (Scheme 4), devoid of the S–S bridge, practically behaves in the same way as **26a**.

Peptide- and amino acid-based hydrogels have been used for the *in situ* generation of fluorescent silver nanoclusters at room temperature under sunlight irradiation, conditions more suited to “green chemistry” protocols. The dipeptides Fmoc–Val–Asp–OH<sup>28</sup> (**27**) and Fmoc-protected L-phenylalanine<sup>29</sup> (**28**) were studied by Banerjee *et al.* on separate occasions (Scheme 4). The two compounds form a transparent, stable hydrogel (0.1–0.2% w/v). The preparation of the gel–NPs composites consists of the addition of freshly prepared aqueous AgNO<sub>3</sub> to a solution of the gelator (DMSO in the case of **27**, and water for **28**). Ag(I)-containing transparent hydrogels were immediately formed. Exposure to sunlight generated a light violet colour in few minutes, indicating the reduction of silver ions to silver nanoclusters (broad SPR<sub>max</sub> = 530 nm and 510 nm, for systems made of **27** and **28**, respectively). While such transformation does not lead to significant morphological changes for the gel made of **27**, the formation of Ag nanoclusters within the hydrogel of **28** produces a transition from helical nanofibers to nanovesicles (as observed by HR-TEM and X-ray diffraction, FE-SEM and AFM). Interestingly, the two systems are able to produce stable AgNPs of small size (1–3 nm  $\varnothing$ ) and of narrow size distribution.

The pyridyl bis(urea) gelator **29a**, developed by Steed *et al.* (Scheme 4), is also interesting.<sup>30</sup> Addition of AgBF<sub>4</sub> to a 7:3 THF:water solution of **29a**, followed by sonication, yielded homogeneous gel materials. Exposure to ambient light transformed the material into a AgNPs composite in 1–2 weeks. A detailed systematic study, performed by varying the AgBF<sub>4</sub>:gelator and the THF:water ratios and the ambient light exposure time, led to the following conclusions: (i) the size and size distribution of the AgNPs strongly depended on the AgBF<sub>4</sub>:gelator ratio. While a 1:1 ratio produces small particles (2–6 nm  $\varnothing$ , SPR<sub>max</sub> = 430 nm) which were clearly attached to the gel fibers (Fig. 3a), increasing the initial AgBF<sub>4</sub> loading leads to larger particles (5–50 nm  $\varnothing$  up to 100 nm  $\varnothing$ ) which showed signs of particle aggregation; (ii) a 1.5 AgBF<sub>4</sub>:gelator ratio seems to be optimal for the structural stability of the gel materials. Compound **29b** (Scheme 4), devoid of the donor N atom on the central ring, does not form any gel material under the same experimental conditions. This strongly hints at the active role of all three pyridyl rings on **29a** in forming the AgNPs materials.

Heterocyclic–metal coordination was also applied in another study described by Kimura *et al.*<sup>31</sup> Here, the self-assembly of the imidazole-containing polycyclic aromatic **30** leads to gel materials in 2-methoxyethanol (Scheme 4). The addition of a solution of AgNO<sub>3</sub> to the gel material in the dark produced a novel gel species, where coordination of the Ag(I) ions to the imidazole units took place (as evidenced by <sup>1</sup>H-NMR, MALDI-TOF and the fluorescence quenching of the initial emitting gel). UV light irradiation transformed the material. TEM imaging (Fig. 3b) revealed the presence of gel fibers nicely decorated with abundant AgNPs (8 nm  $\varnothing$ , SPR<sub>max</sub> = 400–700 nm).

Finally, the following examples demonstrate cases in which an external reducing agent is employed for the reduction of

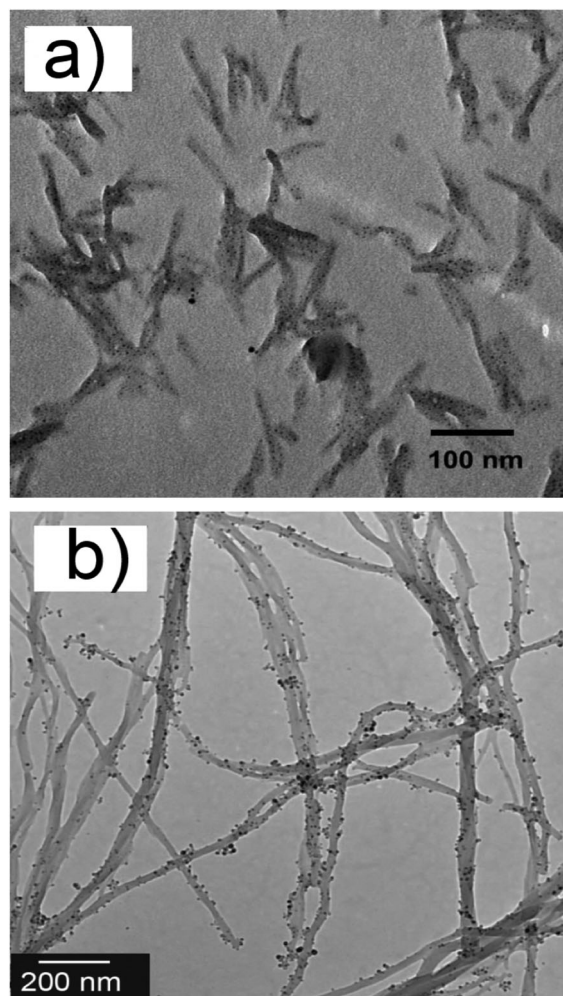
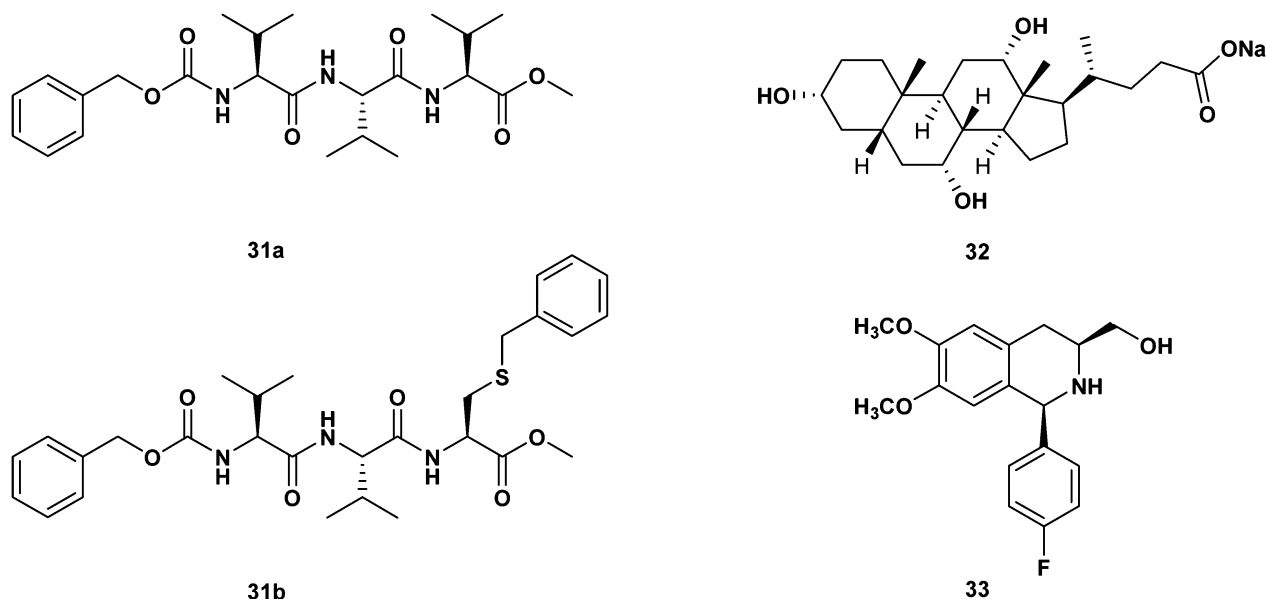


Fig. 3 TEM images of NPs–gel systems: (a) AgNPs in the gel made of a 1:1 AgBF<sub>4</sub>:**29a** mixture, after exposure to light, from ref. 30; (b) AgNPs deposited over the fibers of **30**, from ref. 31, kindly provided by Prof. M. Kimura.

silver and gold cations to elemental species. Taubert and co-workers<sup>32</sup> successfully synthesized an AgNPs–gel system by using mixtures of **31a** and **31b** (Scheme 5). Two-component LMWG systems<sup>33</sup> represent a less frequently used approach for gel preparation, which hinges on the use of two pro-gelator molecules capable of forming a gel only in the presence of each other. This is the case for the two tri-peptides **31a** and **31b**. By varying the molar ratio of the two components, modulation of the properties of the material can be achieved. The two tri-peptides consist of a Val–Val–Val and a Val–Val–Cys sequence, respectively, and the results show that the NPs assembly was controlled by the fraction of cysteine-containing gelator present within the gel system. The reduction of AgNO<sub>3</sub> was accomplished in a hot *n*-butanol solution of the oligopeptides by addition of DMF. The latter species is known to reduce silver ions to metallic silver even at room temperature.<sup>34</sup> Cooling afforded a gel material embedded with AgNPs. Interestingly, the shape and size of the AgNPs could be tuned by varying the **31a**:**31b** ratio. While small spherical particles were obtained at



Scheme 5 Molecular formulae for compounds **31–33**.

higher doses of **31b** (9 nm  $\varnothing$ ), larger particles with complex shapes (plate-like and raspberry-like) were obtained at lower contents of **31b** (> 100 nm  $\varnothing$ ). XPS and SERS studies indicated a strong interaction between the S atom of the cysteine residue of **31b** with silver, a feature absent in the case of tri-peptide **31a**.

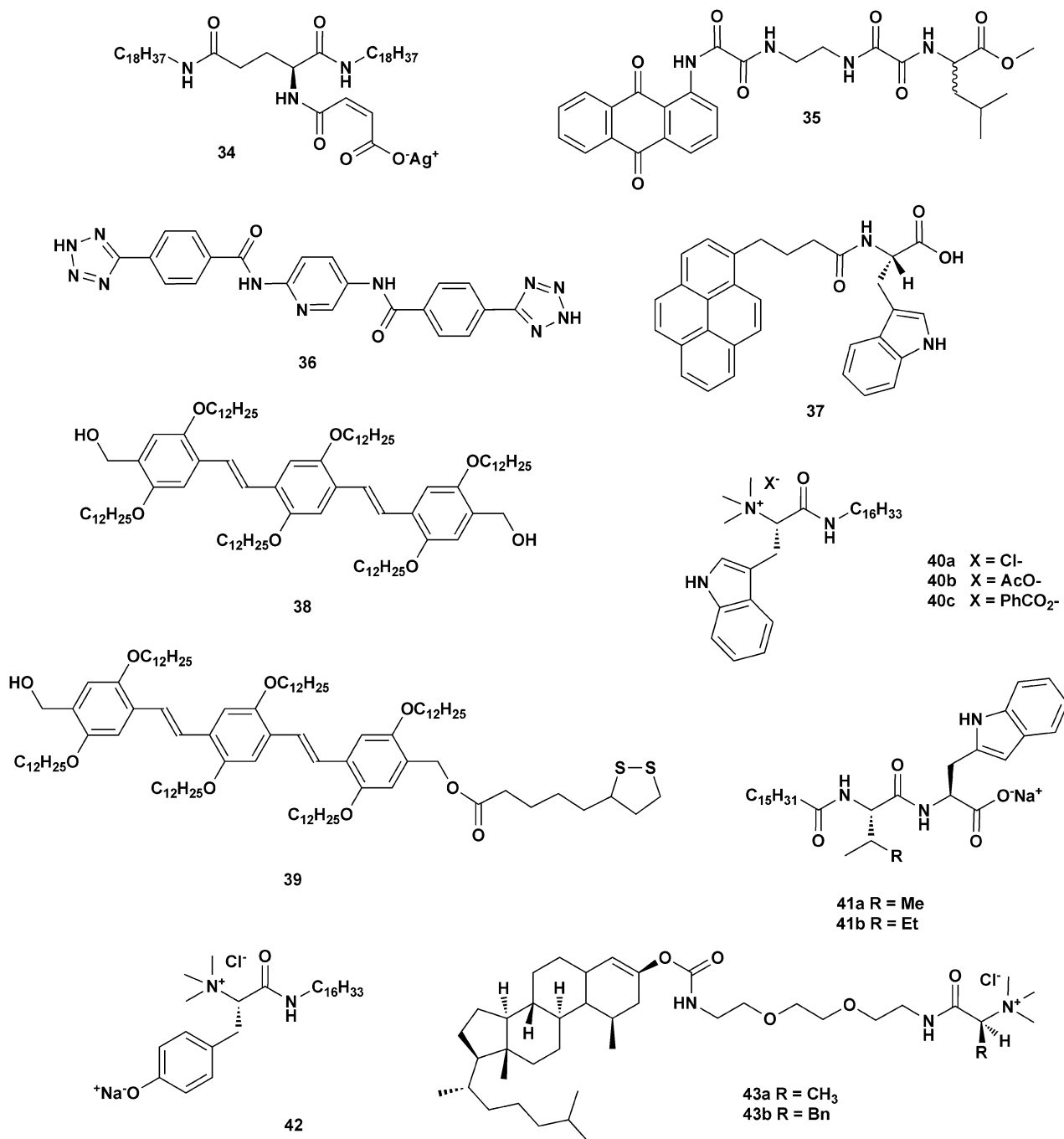
Maitra and co-workers studied the Ca(II)-induced gel formation by sodium cholate, **32** (Scheme 5) for the preparation of AgNPs–gel and AuNPs–gel materials.<sup>35</sup> The AuNPs in the hydrogel were generated *in situ* by doping the calcium cholate hydrogel with AuCl<sub>3</sub> salt, and slowly diffusing sodium cyanoborohydride through the hydrogel. The reduction of Au(III) to AuNPs produced a magenta-coloured material (SPR<sub>max</sub> = 490 nm). Notably, the molar ratio between Ca(II) and Au(III) ions was found to play an important role in the control of agglomeration and the rheological properties of AuNPs–gel hybrid, which could probably be attributed to the competition between the two metals for coordinating the carboxylate groups in **32**. Similarly, when a Ag(I)-doped calcium cholate hydrogel was prepared and treated with sodium cyanoborohydride solution, a yellowish brown hydrogel material containing AgNPs was obtained (SPR<sub>max</sub> = 415 nm). TEM images revealed the presence of Ag-NPs and Au-NPs (1.5–2 nm  $\varnothing$ ), mainly distributed on the junction zones between gel fibres.

Kang, Gao and co-workers<sup>36</sup> developed a cyclic  $\beta$ -amino-alcohol gelator **33** (Scheme 5) derived from 1,2,3,4-tetrahydroisoquinoline and capable of gel formation in various aprotic solvents. The toluene gel of **33** exhibits enhanced stability towards metal ions and quaternary ammonium salts such as tetraoctylammonium chloroaurate ((TOA)AuCl<sub>4</sub>) with respect to its non-fluorinated analogue. This feature becomes relevant in the preparation of AuNPs–gel materials. Indeed, addition of the gelator **33** to a (TOA)AuCl<sub>4</sub> solution in toluene, followed by heating, yielded upon cooling a gel and a colour change, from red to colourless, due to the reduction of Au(III) to

Au(I). Further reduction of Au(I) to Au(0) was achieved by allowing the material to react with aqueous NaBH<sub>4</sub>. This example represents an “intermediate” case, where the reduction is achieved only partially by the gelator and an external reducing agent is needed. TEM images of the AuNPs-containing xerogel show the presence of spherical NPs (5–9 nm  $\varnothing$ ) arranged along the gel fibers. Strong interactions between Ag(I) cations and fluorine atoms are suggested to be responsible for the fast disruption of the material upon addition of silver ions.

### 3. Applications

The rich diversity of systems which can be employed as structural basis for the incorporation of NPs and, thus, generate novel materials, fully extends into ample opportunities for the development of practical applications. One of the most intriguing consequences of the integration of gels constitutional features with the intrinsic properties of metal NPs is represented by the exchange of structural information between objects of different scales. From this point of view, NPs–gel systems based on LMWG systems seem to be definitely superior since, as mentioned above, they permit the design of the material’s internal structure to quite some extent. Frequently, LWMGs contain a chiral center and it is well known that this structural feature can be translated from the molecular level to the nano- and micro-scale during the self-assembly process. Self-assembled fibrillar objects, such as rods, tapes or tubes, can be helically twisted, coiled, or wound around one another to give multiple helices or even coiled coils. These structures might be intrinsically chiral and, consequently, possess a right- or left-handedness. The incorporation of metals into such superstructures could translate the chiral features of the gelator



Scheme 6 Molecular formulae for compounds 34–43.

superstructure to the embedded nano-objects. Not only that, the spatial distribution of NPs can be directed by the gelator's structural properties. This can be of crucial importance in optoelectronic materials. In particular, SPR effects are critically determined not only by the shape and size of the NPs, but also by their arrangement and local dielectric environment.<sup>37</sup> Attempts in this direction are starting to appear in the literature. For example, the Ag(I)-coordinated metallo-gelator, 34 (Scheme 6) was employed to prepare a composite material made of chiral AgNPs entrapped into the organogel.<sup>38</sup> In this case, hydroquinone was used as

reducing agent. The chirality of the resulting NPs embedded in the gel (10–20 nm  $\varnothing$ ) was inferred by the observation of a strongly bisignated circular dichroism (CD) spectrum (negative and positive maxima at 398 nm and 442 nm, respectively). The chirality of the nanoparticles originated and was transferred to the NPs from the chiral gel fibers rather than from the individual gelator molecules. Indeed, the gel state is essential for imparting chirality to the NPs which, when prepared from solution, do not show any sign of chirality. The use of intrinsically chiral NPs is one way of obtaining optical activity at the nanoscale.

A different concept, which is simple and effective, was based on the use of pre-assembled fibrous materials obtained by adding preformed NPs into a fluid dispersion of the chiral anthraquinone-based oxalamide gelators **35** (*R* and *S*, Scheme 6).<sup>39</sup> The self-assembled fibers served as chiral templates for a 3D arrangement of gold nanorods (NRs) into the hybrid materials, thus transferring the chirality from the fibers to the NPs. Indeed, CD measurements revealed an intense plasmon-induced Cotton effect (*R* and *S* derivatives) with strong anisotropy. Notably, spherical NPs show no such behavior, indicating the crucial role of the NP's shape.

Achieving catalysis by means of NPs-gel systems is quite an appealing idea. Noble metals such as Ag and Au are used for catalysis in numerous important chemical transformations.<sup>40</sup> To achieve a high performance at a low cost, precious catalysts are required to have a large surface-volume ratio. Hence, NPs are highly attractive species to serve as catalysts and their incorporation into gel networks might represent a winning strategy in catalyst design.

Two notable examples exist in the literature. The non-symmetric bis-tetrazole based ligand **36**, described by Lee, Jung and co-workers,<sup>41</sup> is able to form a gel in water under basic pH conditions in the presence of AgNO<sub>3</sub> or AgClO<sub>4</sub> salts. Over time, a progressive change of the gel colour, from white to brown, along with TEM images, proved the reduction of the Ag(I) cation to metallic AgNPs within the gel material. The data also show that the size distribution of the NPs can be modulated by changing the gelator:Ag salt ratio (1–3 nm  $\varnothing$  for a 1:2 ratio, 2–5 nm  $\varnothing$  for a 1:4 ratio). The catalytic activity of the new material was examined by investigating the reduction of a simple model compound, 4-nitrophenol (4NP) to 4-aminophenol (4AP). The test was performed by percolating a solution containing 4NP and NaBH<sub>4</sub> through a glass column filled with the AgNPs-gel material. It is well known that the 4NP to 4AP conversion in the presence of NaBH<sub>4</sub> is thermodynamically favoured but kinetically slow, and this transformation is often chosen as a model reaction for testing the catalytic activity of various metallic species.<sup>42</sup> The NPs-gel system based on **36** affords the desired product with high yield, and no alteration of the catalytic material was detected. An electron-relay mechanism, in which electron transfer from the hydride to the substrate is mediated by the AgNPs, was suggested, in line with previous studies.<sup>43</sup>

In Banerjee's laboratory, a three component hybrid material composed of a gel matrix containing both graphene oxide (GO) fragments and gold NPs has been created and studied.<sup>44</sup> The key ingredient is the hydrogelator molecule, the pyrene-conjugated tryptophan based compound **37**. The intrinsic gelating properties of **37** in phosphate buffered solution are dependent on the presence of large surface aromatics and a Trp group, which are both crucial features. As shown, the pyrene unit is capable of establishing interactions with the flat GO fragments, while the Trp group allows for the *in situ* formation of gold NPs. The morphology of the tri-hybrid hydrogel studied by TEM and FE-SEM revealed the coexistence of three distinctly different nanostructures: nanofibers, nanosheets and nanoparticles, deriving from the self-assembly of **37**, the GO and

the AuNPs, respectively. The catalytic activity was tested for the reduction of the aromatic nitro group of 4NP and 4-nitroaniline (4NA) in the presence of NaBH<sub>4</sub>. The authors compared this tri-hybrid material with a hybrid AuNPs composite obtained by an *in situ* process between **37** and Au(III) ions. The latter system would be *per se* rightfully part of the collection of examples in this review, being itself a novel AuNPs gel system. However, its catalytic properties are indeed surpassed by those of the tri-hybrid system, thus proving the successful synergy between the GO and the AuNPs within the hydrogel matrix. A comparison between the novel catalytic systems here described with other systems reported in the literature is limited due to the lack of experimental details, especially on the kinetic model assumed, which is needed to extract reliable quantitative information from the kinetic data.<sup>43</sup>

Novel optical properties emerge in the novel linear hybrid system in which AuNPs are bound to  $\pi$ -conjugated oligo-(*p*-phenylenevinylene) (OPV) supramolecular aggregates, as described by Meskers, Schenning and co-workers.<sup>45</sup> The authors employed the gelator molecule **38** (Scheme 6) in toluene as a scaffold for the spatial organization of AuNPs capped with the derivative **39** (obtained by the introduction of a disulfide moiety in **38**). The AuNPs capped with **39** interact with the gel materials made of **38**, also influencing its critical gelation concentration (cgc). More importantly, as shown by the TEM images, the NPs are found to align on both sides of gel tapes – 40 nm wide and 7 nm high (minimum detected) – giving rise to a hybrid material. Such alignment was not induced by the drying effect, and cryo-TEM images confirmed the distribution of the NPs in the composite.

The spectroscopic data on the novel material confirm the electronic communication between the gel tapes made of **38** and the **39**-AuNPs, since the fluorescence of OPV derivative **38** was considerably quenched in the hybrid material – the emission intensity was reduced by a factor of 33 in comparison with the emission intensity of **38** alone – with a concomitant decrease in its lifetime. Photoinduced absorption (PIA) studies confirmed the presence of a dynamic process that takes place on a nanosecond time scale and involves the diffusion of electronic excitations through the tape toward the AuNPs.

Another application of NPs-gel materials derives from the fact that silver and silver NPs have been known since Roman times to possess antimicrobial activity, and their use in the healthcare industry is nowadays well established.<sup>46</sup> In general, AgNPs are routinely found to be more effective against Gram-negative bacteria than Gram-positive ones and, for this reason, the work done by Das and co-workers<sup>47</sup> on the use of AgNPs-gel materials with high antimicrobial activity is particularly interesting.

Following various *in situ* procedures, compounds **40a-c**, **41a-b**, **42** and **43a-b** (Scheme 6), can afford AgNPs-gel materials.

Table 1 summarizes the antimicrobial activity of the AgNPs gel composites made with **40**–**43**, with the minimum inhibitory concentration (MIC) calculated referring to the gelator concentration and to the metal concentration (in parentheses). As can be clearly seen, the effectiveness of the activity observed spans

**Table 1** Minimum inhibitory concentration ( $\mu\text{g mL}^{-1}$ ) expressed as gelator concentration and silver concentration (in parenthesis) for the AgNPs–gel systems based on **40–43** in against Gram-positive (+) and Gram-negative (–) bacteria<sup>47</sup>

	+		–	
	<i>B. subtilis</i>	<i>S. aureus</i>	<i>E. coli</i>	<i>K. aerogens</i>
<b>40a</b>	20 (7.4)	10 (3.7)	60 (22.2)	80 (29.6)
<b>40b</b>	3	2	100	20
<b>40c</b>	5	2	50	25
<b>41a</b>	100 (56)	150 (84)	150 (84)	75 (42)
<b>41b</b>	200 (74)	200 (74)	200 (74)	100 (37)
<b>42</b>	20 (7.8)	10 (2.8)	75 (21)	55 (15.4)
<b>43a</b>	70	50	100	75
<b>43b</b>	30	20	60	50

over two orders of magnitude of concentration but, in general, the nanocomposites exhibited excellent antibacterial activity against both Gram-positive and Gram-negative bacteria. In some of the most effective cases, for **40a** and especially for **40b–c**, the increase in efficacy is remarkably high, between *ca.* 10- to 50-fold. These data can be compared, although only qualitatively, with those reported for various AgNP suspensions,<sup>48</sup> and it must be noted that compounds **40a–c** already showed antimicrobial activity *per se*.<sup>47b</sup>

## 4. Conclusions

To paraphrase the famed French scientist Berthelot, chemistry has the unparalleled privilege, unique among other sciences, to create its own subject. This prerogative translates into virtually infinite opportunities for the discovery of novel species and materials. This concept applies well in the case of NPs–gel hybrid materials.

Despite extensive investigation of both the supramolecular chemistry of LMWGs and the preparation and physico-chemical properties of noble NPs, the integration of these components into a single entity represents a very recent and highly welcome novelty in the field of functional, smart materials.

This review intends to display the works at the *avant garde* on the developments of noble metal NPs–gel systems. These materials originate from the combination of objects belonging to different scale domains. Micrometer-scaled fibers, created by the self-assembly of gelator monomers, interact with nanoclusters of noble metals, in what eventually makes up a macroscopic object. Such inter-domain crossing is reckoned to be of great and increasing importance in supramolecular and materials chemistry and, undoubtedly, will enable advances in both fields.

Noble metal NPs–gels hybrids can be obtained by several different procedures and their features can be characterized *inter alia* by a combination of electronic microscopy (SEM, TEM, *etc.*) and UV-vis spectroscopy. Both the preparation and characterization of NPs–gel materials are described in this review. In particular, we put strong emphasis in the description of the various synthetic pathways, which are grouped into two

different categories: type I and type II, depending on whether the NPs are formed prior to the material formation or by an *in situ* process. The many variables involved in the preparation of NPs–gel materials and the lack of a comprehensive and accepted view on the influence of the preparation on the final properties of the material demands attention.

Although many of the works surveyed here focus on the study of the effect that one of the components may exert on the other, in terms of both structural and/or optical features, we believe that these new materials can be indeed considered entities in their own right. As mentioned above, the exploitation of their novel emerging properties could engender remarkable developments and some applications have already been reported. NPs–gel materials have indeed been tested as novel catalysts, as antimicrobial supports, and for the construction of chiral optical materials. Despite these applied developments, the research on this topic, so far, has had many features in common with the exploration of a *terra incognita*, and many aspects of the integration of NPs into gel materials are not completely understood. In particular, attention should be paid to identifying whether the presence of NPs can contribute additional stabilization of the gel matrix or not, and, eventually, to what extent. The mode of NPs–gel hybrid preparation (pre-formed NPs or *in situ* generated NPs) is obviously relevant to this issue. Also, the influence of the presence of NPs on the self-assembly process of the gelator is not yet completely understood, let alone the role of the formation process of the NPs on the resultant material properties. For example, although some authors believe that *in situ* NPs formation could allow for the retention of the original gelator self-assembly process, the data collectively reviewed here strongly indicate quite a variability of behavior, depending on the identity of the gelator species and the experimental conditions employed.

Although in its early stages of development, and despite many fundamental questions that still remain unanswered, NPs–gel materials represent a promising field of research and we expect a thriving future ahead.

## Acknowledgements

M.C. gratefully acknowledges the Programma per Giovani Ricercatori “Rita Levi Montalcini” 2009.

## Notes and references

- (a) X. Yan, F. Wang, B. Zheng and F. Huang, *Chem. Soc. Rev.*, 2012, **41**, 6042–6065; (b) K. Ariga, H. Ito, J. P. Hill and H. Tsukube, *Chem. Soc. Rev.*, 2012, **41**, 5800–5835; (c) G. R. Whittell, M. D. Hager, C. S. Schubert and I. Manners, *Nat. Mater.*, 2011, **10**, 176–188.
- (a) C. N. R. Rao, G. U. Kulkarni, P. J. Thomas and P. P. Edwards, *Chem. Soc. Rev.*, 2000, **29**, 27–35; (b) P. K. Jain, X. Huang, I. H. El-Sayed and M. A. El-Sayed, *Acc. Chem. Res.*, 2008, **41**, 1578–1586; (c) S. Eustis and M. A. El-Sayed, *Chem. Soc. Rev.*, 2006, **35**, 209–217; (d) R. Jin, *Nanoscale*, 2010, **2**, 343–362; (e) Y. Yao, M. Xue, Z. Zhang, M. Zhang, Y. Wang and F. Huang, *Chem. Sci.*, 2013, **4**, 3667–3672.
- (a) A. M. Alkilany, S. E. Lohse and C. J. Murphy, *Acc. Chem. Res.*, 2013, **46**, 650–661; (b) K. Saha, S. S. Agasti, C. Kim, X. Li and V. M. Rotello, *Chem. Rev.*, 2012, **112**, 2739–2779; (c) H. Jans and Q. Huo, *Chem. Soc. Rev.*, 2012, **41**, 2849–2866.

- 4 P. Sciau, Nanoparticles in Ancient Materials: The Metallic Lustre Decorations of Medieval Ceramics, in *The Delivery of Nanoparticles*, ed. A. A. Hashim, InTech, 2012.
- 5 P. A. Gale and J. W. Steed, *Supramolecular Chemistry: From Molecules to Nanomaterials*, Wiley-VCH, 2012.
- 6 (a) *Molecular Gels: Materials with Self-Assembled Fibrillar Networks*, ed. R. G. Weiss and P. Terech, Springer, Dordrecht, The Netherlands, 2005; (b) S. Dong, B. Zheng, D. Xu, X. Yan, M. Zhang and F. Huang, *Adv. Mater.*, 2012, **24**, 3191–3195; (c) M. Zhang, D. Xu, X. Yan, J. Chen, S. Dong, B. Zheng and F. Huang, *Angew. Chem., Int. Ed.*, 2012, **51**, 7011–7015; (d) X. Yan, D. Xu, X. Chi, J. Chen, S. Dong, X. Ding, Y. Yu and F. Huang, *Adv. Mater.*, 2012, **24**, 362–369; (e) S. Dong, Y. Luo, X. Yan, B. Zheng, X. Ding, Y. Yu, Z. Ma, Q. Zhao and F. Huang, *Angew. Chem., Int. Ed.*, 2011, **50**, 1905–1909.
- 7 B. Rybtchinski, *ACS Nano*, 2011, **5**, 6791–6818.
- 8 *PolymERIC and Self Assembled Hydrogels: From Fundamental Understanding to Applications*, ed. X. J. Loh and O. A. Scherman, Monogr. Supramol. Chem., series ed. P. Gale and J. Steed, RSC Publishing, 2013.
- 9 (a) P. Terech and R. G. Weiss, *Chem. Rev.*, 1997, **97**, 3133–3159; (b) S. Banerjee, R. K. Das and U. Maitra, *J. Mater. Chem.*, 2009, **19**, 6649–6687; (c) M.-C. Daniel and D. Astruc, *Chem. Rev.*, 2004, **104**, 293–346.
- 10 There are a number of classical methods for the synthesis of nanoparticles. Some are: (i) the Brust method; (ii) the Turkevich method; (iii) the Perrault method; see also ref. 9; for AgNPs, see (a) P. Graf, A. Manton, A. Foelske, A. Shkilnyy, A. Mašić, A. F. Thünemann and A. Taubert, *Chem. - Eur. J.*, 2009, **15**, 5831–5844, and references therein; (b) B. L. Cushing, V. L. Kolesnichenko and C. J. O'Connor, *Chem. Rev.*, 2004, **104**, 3893–3946.
- 11 A. Caragheorghopol and V. Chechik, *Phys. Chem. Chem. Phys.*, 2008, **10**, 5029–5041.
- 12 M. Kimura, S. Kobayashi, T. Kuroda, K. Hanabusa and H. Shirai, *Adv. Mater.*, 2004, **16**, 335–338.
- 13 I. A. Coates and D. K. Smith, *J. Mater. Chem.*, 2010, **20**, 6696–6702.
- 14 S. Bhat and U. Maitra, *Chem. Mater.*, 2006, **18**, 4224–4226.
- 15 (a) S. Bhattacharya, A. Srivastava and A. Pal, *Angew. Chem., Int. Ed.*, 2006, **45**, 2934–2937; (b) A. Pal, A. Srivastava and S. Bhattacharya, *Chem. - Eur. J.*, 2009, **15**, 9169–9182.
- 16 J. Nanda, B. Adhikari, S. Basak and A. Banerjee, *J. Phys. Chem. B*, 2012, **116**, 12235–12244.
- 17 N. M. Sangeetha, S. Bhat, G. Raffy, C. Belin, A. Loppinet-Serani, C. Aymonier, P. Terech, U. Maitra, J.-P. Desvergne and A. Del Guerzo, *Chem. Mater.*, 2009, **21**, 3424–3432.
- 18 H. Erdogan, H. Sakalak, M. S. Yavuz and G. Demirel, *Langmuir*, 2013, **29**, 6975–6982.
- 19 (a) P. K. Vemula and G. John, *Chem. Commun.*, 2006, 2218–2220; (b) P. K. Vemula, U. Aslam, V. A. Mallia and G. John, *Chem. Mater.*, 2007, **19**, 138–140.
- 20 S. Ray, A. K. Das and A. Banerjee, *Chem. Commun.*, 2006, 2816–2818.
- 21 R. N. Mitra and P. K. Das, *J. Phys. Chem. C*, 2008, **112**, 8159–8166.
- 22 T. Kar, S. Dutta and P. K. Das, *Soft Matter*, 2010, **6**, 4777–4787.
- 23 D. Das, S. Maiti, S. Brahmachari and P. K. Das, *Soft Matter*, 2011, **7**, 7291–7303.
- 24 S. Chatterjee and A. K. Nandi, *Chem. Commun.*, 2011, **47**, 11510–11512.
- 25 M. Sakamoto, M. Fujistuka and T. Majima, *J. Photochem. Photobiol., C*, 2009, **10**, 33–56.
- 26 C. S. Love, V. Chechik, D. K. Smith, K. Wilson, I. Ashworth and C. Brennan, *Chem. Commun.*, 2005, 1971–1973.
- 27 K. Torigoe and K. Esumi, *Langmuir*, 1992, **8**, 59–63.
- 28 B. Adhikari and A. Banerjee, *Chem. - Eur. J.*, 2010, **16**, 13698–13705.
- 29 S. Roy and A. Banerjee, *Soft Matter*, 2011, **7**, 5300–5308.
- 30 M.-O. M. Piepenbrock, N. Clark and J. W. Steed, *Soft Matter*, 2011, **7**, 2412–2418.
- 31 M. Kimura, T. Hatanaka, H. Nomoto, J. Takizawa, T. Fakawa, Y. Tatewaki and H. Shirai, *Chem. Mater.*, 2010, **22**, 5732–5738.
- 32 A. Manton, A. G. Guex, A. Foelske, L. Mirolo, K. M. Fromm, M. Painsi and A. Taubert, *Soft Matter*, 2008, **4**, 606–617.
- 33 (a) L. E. Buerkle and S. J. Rowan, *Chem. Soc. Rev.*, 2012, **41**, 6089–6102; (b) A. R. Hirst and D. K. Smith, *Chem. - Eur. J.*, 2005, **11**, 5496–5508.
- 34 I. Pastoriza-Santos and L. M. Liz-Marzán, *Langmuir*, 1999, **15**, 948–951.
- 35 A. Chakrabarty, U. Maitra and A. D. Das, *J. Mater. Chem.*, 2012, **22**, 18268–18274.
- 36 Y. Xu, C. Kang, Y. Chen, Z. Bian, X. Qiu, L. Gao and Q. Meng, *Chem. - Eur. J.*, 2012, **18**, 16955–16961.
- 37 M. E. Stewart, C. R. Anderton, L. B. Thompson, J. Maria, S. K. Gray, J. A. Rogers and R. G. Nuzzo, *Chem. Rev.*, 2008, **108**, 494–521.
- 38 Y. Li and M. Liu, *Chem. Commun.*, 2008, 5571–5573.
- 39 A. Guerrero-Martínez, B. Auguie, J. L. Alonso-Gomez, Z. Džolić, S. Gomez-Grana, M. Žinić, M. M. Cid and L. M. Liz-Marzán, *Angew. Chem., Int. Ed.*, 2011, **50**, 5499–5503.
- 40 (a) Z. Li, C. Brouwer and C. He, *Chem. Rev.*, 2008, **108**, 3239–3265; (b) M. Naodovic and H. Yamamoto, *Chem. Rev.*, 2008, **108**, 3132–3148.
- 41 J. H. Lee, S. Kang, J. Y. Lee and J. H. Jung, *Soft Matter*, 2012, **8**, 6557–6563.
- 42 (a) S. Sarkar, A. K. Guria and N. Pradhan, *Chem. Commun.*, 2013, **49**, 6018–6020; (b) Z. D. Pozun, S. E. Rodenbusch, E. Keller, K. Tran, W. Tang, K. J. Stevenson and G. Henkelman, *J. Phys. Chem. C*, 2013, **117**, 7598–7604; (c) Y. Lin, Y. Qiao, Y. Wang, Y. Yan and J. Huang, *J. Mater. Chem.*, 2012, **22**, 18314–18320; (d) N. Pradhan, A. Pal and T. Pal, *Langmuir*, 2001, **17**, 1800–1802.
- 43 S. Wunder, Y. Lu, M. Albrecht and M. Ballauff, *ACS Catal.*, 2011, **1**, 908–916.
- 44 J. Nanda, A. Biswas, B. Adhikari and A. Banerjee, *Angew. Chem., Int. Ed.*, 2013, **52**, 5041–5045.
- 45 J. van Herrikhuyzen, S. J. George, M. R. J. Vos, N. A. J. M. Sommerdijk, A. Ajayaghosh, S. C. J. Meskers and A. P. H. J. Schenning, *Angew. Chem., Int. Ed.*, 2007, **46**, 1825–1828.
- 46 (a) J.-Y. Maillard and P. Hartemann, *Crit. Rev. Microbiol.*, 2013, **39**, 373–383; (b) L. Rizzello and P. Pompa, *Chem. Soc. Rev.*, 2014, **43**, 1501–1518.
- 47 (a) A. Shome, S. Dutta, S. Maiti and P. K. Das, *Soft Matter*, 2011, **7**, 3011–3022; (b) S. Dutta, A. Shome, T. Kar and P. K. Das, *Langmuir*, 2011, **27**, 5000–5008; (c) S. Dutta, A. Shome, S. Debnath and P. K. Das, *Soft Matter*, 2009, **5**, 1607–1620; (d) S. Dutta, T. Kar, D. Mandal and P. K. Das, *Langmuir*, 2013, **29**, 316–327.
- 48 (a) Q. H. Tran, V. Q. Nguyen and A.-T. Le, *Adv. Nat. Sci.: Nanosci. Nanotechnol.*, 2013, **4**, 033001; (b) A. K. Suresh, D. A. Pelletier and M. J. Doktycz, *Nanoscale*, 2013, **5**, 463–474.